JOURNAL OF MATERIALS SCIENCE 33 (1998) 2283–2297

Incipient melting of $Al_5Mg_8Si_6Cu_2$ and Al_2Cu intermetallics in unmodified and strontium-modified Al–Si–Cu–Mg (319) alloys during solution heat treatment

F.H. SAMUEL
Département des Sciences appliquées, Université du Québec à Chicoutimi, 555 boul. de l'Université, Chicoutimi (Québec), Canada G7H 2B1

The present work was performed on seven alloys containing in common Al–6.5 wt %Si–3.5 wt % Cu, with magnesium in the range 0.04–0.45 wt %, and strontium in the range 0–300 p.p.m. The alloys were cast in the form of tensile test bars, solution heat treated in the temperature range 480–540 °C for times up to 24 h. Two types of solution heat treatment were applied: (i) single-stage, where the test bars were solution treated at a certain temperature for 12 h prior to quenching in hot water (60 °C); (ii) two-stage, where the test bars were solution treated for 12 h/510 °C + 12 h/T °C (T = 510, 520, 530, 540 °C), followed by quenching in hot water. In the low-magnesium alloys (i.e. with Mg ~ 0.04 wt %), melting of the Al_2Cu phase commenced at 540 °C. Increasing the magnesium content to ~0.5 wt % reduced the incipient melting temperature of the $Al_5Mg_8Si_6Cu_2$ phase to 505 °C. The mechanism of incipient melting and its effect on the tensile properties have been discussed in detail. © *1998 Chapman & Hall*

1. Introduction

The excellent castability and mechanical properties of type 319 alloy make it a popular foundry alloy for automotive applications. Based on the Al–Si system, the alloy contains copper and magnesium as the main alloying elements, together with varying amounts of iron, manganese and zinc as impurity elements. These elements partly go into solid solution in the matrix and partly form intermetallic particles during solidification.

Following casting, solution heat treatment is routinely carried out to maximize the concentration of the age-hardening constituent (Mg_2Si) in solid solution, to homogenize the casting, and to alter the structure of the eutectic silicon particles in order to improve the mechanical properties. Control of the solution-treatment temperature is very critical because, if the melting point is exceeded, there is localized melting at the grain boundaries and the mechanical properties are reduced [1]. The solidification sequence in 319 alloy as reported by Backerud *et al.* [2] is listed in Table I. The $Al_5Mg_8Cu_2Si_6$ and Al_2Cu intermetallics are expected to melt at 507 and 525 °C, respectively.

Most of the recommended heat treatments of Al–Si–Cu alloys [3] restrict the solution temperature below the final solidification point in order to avoid the melting of copper-containing phases. This phenomenon was studied by Reiso *et al.* [4, 5] in Al–Cu systems. Their results show that melting takes place at and above the corresponding eutectic temperature due to reductions in the Gibbs free energies. Non-equilibrium heat treatment was suggested by Awano and Shimizu [6] for Al–7 wt % Si–3 wt % Cu alloy. This treatment involves solution treatment at temperatures slightly higher than the final solidification temperature of (Al + Al_2Cu) eutectic. This process is expected to enhance dissolution of Al_2Cu in the aluminium matrix.

Temporary overheating, i.e. with respect to the melting point, is known to lead to void formation [7]. Another phenomenon may also cause microvoid formation. The soluble phases containing magnesium have a tendency to leave behind microvoids when they dissolve, especially when the particles are large and the heating rate is fast. This has been attributed to a density difference between particle and matrix and insufficient time for the aluminium atoms to back diffuse into the volume fomerly occupied by the particle. The effect is more detrimental if these voids are combined with high-temperature oxidation [8].

The present work summarizes the important observations made on the dissolution and melting of the copper-base intermetallics during solution heat treatment of 319-type alloys. The study was performed on seven alloys. These alloys were classified into two main categories, depending on the magnesium concentration, namely Al–Si–Cu (Mg $\leqslant$ 0.06 wt %) and Al–Si–Cu–Mg (Mg ~ 0.3–0.5 wt %). These investigations represent part of an ongoing research programme established at the Université du Québec

à Chicoutimi on the heat treatment of Al–Si alloys and their composites for automotive applications [9–16].

2. Experimental procedure

The chemical compositions of the as-received alloys (coded A, G and W) are shown in Table II (other codes correspond to Mg and Sr additions made to these alloys). The ingots were melted and cast in a Stahl permanent mould (type ASTM B-108) heated at 400 °C. The melt hydrogen level in all cases was ~0.08 ml/100 g Al just prior to casting. Magnesium was added as pure metal using a perforated graphite bell. Complete details of the melting and casting procedure are given elsewhere [9]. Castings were also made in a cylindrical metallic mould (2.5 cm diameter, 20 cm long).

Test bars (gauge length 5 cm and cross-section diameter 1.27 cm) obtained from the Stahl mould castings were solution heat treated in a forced-air furnace (where the temperature could be controlled to within $\pm$ 1 °C), at a rate of 3.5 °C min^{-1} to the required solution temperature in the range 480–540 °C. The solution times varied between 2 and 24 h. For each individual treatment, at least eight test bars were used. The solution-treated test bars were pulled to fracture at room temperature in an Instron Universal testing machine at a strain rate of 4×10^{-4} s^{-1}. A strain-gauge extensometer was attached to the test bar for measuring the alloy ductility. Samples for dimensional changes study (1.7 cm diameter, 7 cm long) were machined from the cylindrical castings, heat treated similarly, and tested using a special apparatus shown schematically in Fig. 1. Microstructural changes were examined using optical microscopy on polished sample surfaces of metallographic specimens obtained from the solution-treated samples.

Measurements by differential scanning calorimetry (DSC) were carried out on 20 mg powder samples obtained from various solution heat-treated bars, heated up to 675 °C at 10 °C min^{-1}, followed by cooling at the same rate to room temperature. The heating and cooling cycle was carried out under dynamic argon atmosphere.

TABLE I Reactions during solidification of 319.1 alloy at 0.6 °C s^{-1} [2]

Reaction	Suggested temperature (°C)
1. Development of α-Al dendritic network	609
2a. Liq. → Al + $Al_{15}(Mn,Fe)_3$ Si_2	509
2b. Liq. → Al + Al_5FeSi + $Al_{15}(Fe,Mn)_3$ Si_2	509
3. Liq. → Al + Si + Al_5FeSi	575
4. Liq. → Al + Al_2Cu + Si + Al_5FeSi	525
5. Liq. → Al + Al_2Cu + Si + $Al_5Mg_8Cu_2Si_6$	507

TABLE II Chemical compositions (wt %) of the 319 type alloys studied in the present work

Alloy code	Si	Cu	Fe	Mn	Mg	Zn	Ti	Sr
A	6.2	3.2	0.15	0.03	0.3	0.004	< 0.001	< 0.001
G	6.2	3.46	0.35	0.09	0.04	0.04	0.155	–
GM	6.17	3.65	0.35	0.09	0.45	0.04	0.007	–
GMS	6.78	3.74	0.35	0.10	0.60	0.14	0.14	0.0188
GMST	6.48	3.84	0.47	0.13	0.47	0.06	0.17	0.075
W	5.85	3.2	0.80	0.34	0.09	0.45	0.14	–
WM	5.85	3.2	0.8	0.34	0.47	0.45	0.14	–

3. Results and discussion

3.1. DSC runs

Fig. 2a shows the results of a DSC run carried out on a powder sample of unmodified Al–Si–Cu alloy. Melting of the Al_2Cu phase is expected to start when

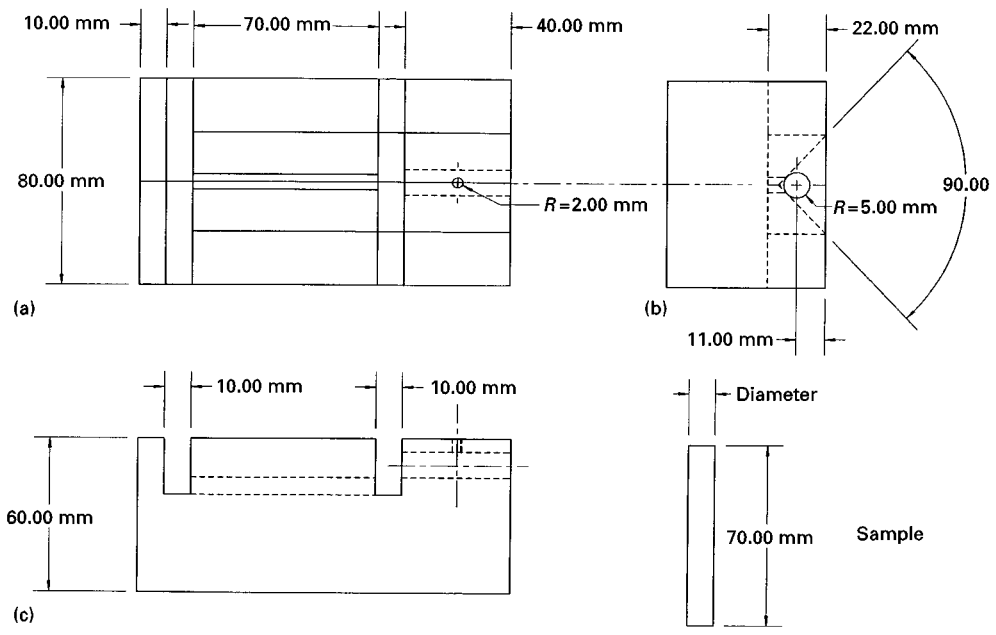

Figure 1 Schematic diagram of the apparatus used for dimensional change measurements.

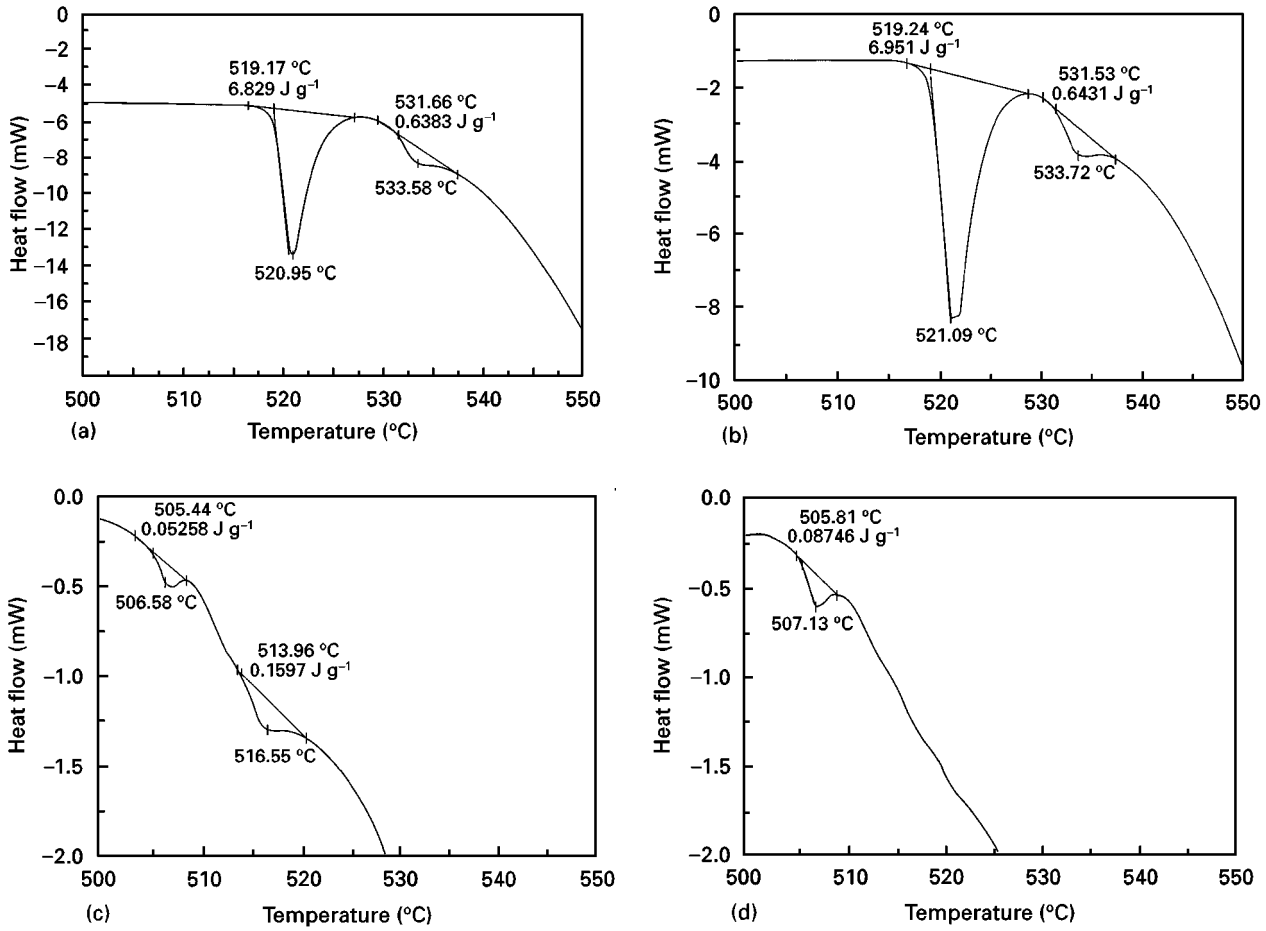

Figure 2 DSC curves obtained from: (a) G alloy, (b) G alloy with 300 p.p.m. Sr, (c) GM alloy, (d) GMS alloy.

TABLE III Average dimensional changes for samples solution treated at 470 °C

Alloy	As-cast length (mm)	Length variation after solution treatment and quenching (mm)	Length variation after ageing (mm)	Total variation (mm)	Total expansion (%)
G	69.86	0.01	0.029	0.039	0.056
GM	69.878	0.027	0.022	0.069	0.10
GMS	69.79	0.019	0.019	0.039	0.056
GMST	69.75	0.021	0.02	0.042	0.06

TABLE IV Average dimensional changes for samples solution treated at 505 °C.

Alloy	As-cast length (mm)	Length variation after solution treatment + quenching (mm)	Length variation after ageing (mm)	Total variation (mm)	Total expansion (%)
G	69.77	0.327	0.044	0.744	1.06
GM	69.68	0.926	0.0285	0.95	1.36
GMS	69.8	1.087	0.008	1.094	1.56
GMST	69.8	0.683	0.038	0.572	0.817

the sample is heated above 520 °C. Below this temperature, the Al_2Cu particles undergo dissolution in the aluminium matrix. These results are in good agreement with those reported by Shivkumar *et al.* [17] for unmodified sand-cast 319 alloy. The copper-phase reactions are not, however, affected in any way by the addition of 300 p.p.m. Sr (i.e. modification), in that the temperature and the energies of the reactions remain the same (Fig. 2b). Addition of ~0.5 wt % Mg to the base alloy, i.e. GM alloy leads to a marked shift in the melting point of the copper phases to a lower temperature, i.e. 505 °C (Fig. 2c). As in the case of the Al–Si–Cu alloy, modification with strontium (i.e. GMS alloy) has no effect on the reactions, Fig. 2d.

3.2. Dimensional changes

Tables III and IV reveal the variation in the length of samples solution treated at 470 and 505 °C, respectively. It is evident that when the samples are solution

treated at 470 °C and quenched, the ageing thereafter has a more pronounced effect on the increase in alloy dimension rather than the solution treatment. In contrast, solution treatment at 505 °C leads to a noticeable growth of the casting, particularly for the high-magnesium alloys, reaching approximately 1.5%. Ageing results in further increase in the alloy dimensions, but at much lesser magnitude compared to that obtained after solution treatment and quenching. The variation in the alloy dimensions is not significantly affected by the addition of strontium.

3.3. Tensile properties

3.3.1. Al–Si–Cu alloys

Fig. 3 shows the amount of undissolved Al_2Cu phase obtained in solution heat-treated samples of G alloy,

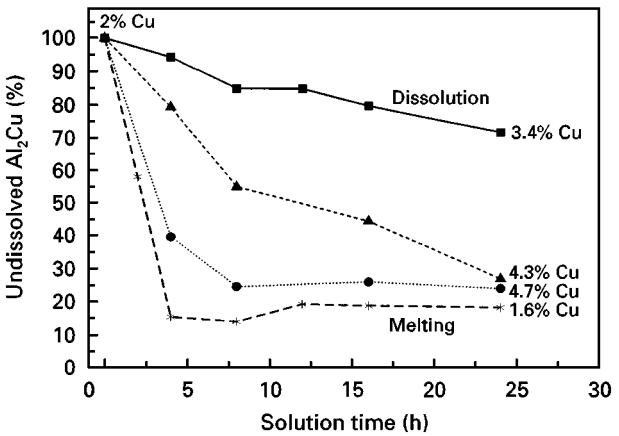

Figure 3 Variation in the percentage of undissolved Al_2Cu as a function of solution time in the temperature range 480–540 °C. (■) 480 °C, (▲) 505 ° C, (●) 515 °C, (*) 540 °C.

calculated as a percentage of the average value obtained in the as-cast condition. The numerical values quoted alongside the 24 h solution-time reading at different solution temperatures indicate the dissolved copper content obtained from electron probe microanalysis (EPMA) for these samples. It is evident that heating at temperatures below the final solidification temperature (i.e. 480 °C) results in a very sluggish dissolution of the Al_2Cu phase. Dissolution of Al_2Cu is accelerated as soon as the solution temperature is increased to 505 °C, where the dissolution exhibits a relatively linear behaviour with solution time. At 515 °C, a temperature recommended for solution heat treatment, about 80% of the Al_2Cu has almost dissolved after 8 h. Further heating at this temperature does not bring about much change in the amount of undissolved Al_2Cu phase. Solution treatment at 540 °C apparently causes a marked change. This, however, is attributed to the melting of the Al_2Cu phase, rather than to its dissolution.

The tensile properties of solution heat-treated test bars are listed in Table V. It is evident that the yield strength (YS) and ultimate tensile strength (UTS) are increased by increasing the solution temperature and further by increasing the solution time. At 540 °C, test bars exhibit premature failure due to melting of the Al_2Cu phase. Plotting the variation in tensile properties, i.e. YS, UTS and percent elongation (El %) (Fig. 4), as a function of the copper concentration in the aluminium matrix in the temperature range 480–515 °C gives linear relationships for which the following equations are obtained

$$\text{YS (MPa)} = 81.1 + 24.9 \times \text{Cu (wt \%)} \quad (1)$$

$$\text{UTS (MPa)} = 15.4.5 + 36.6 \times \text{Cu (wt \%)} \quad (2)$$

$$\text{El (\%)} = 0.023 + 1.01 \times \text{Cu (wt \%)} \quad (3)$$

TABLE V Average tensile properties of solution heat-treated test bars obtained from degassed and filtered melts (G alloy)

Solution temperature (°C)	Solution time (h)	YS (MPa)	UTS (MPa)	EL (%)
480	2	145 ± 12	259 ± 10	3.19 ± 0.5
	4	140 ± 1	269 ± 3	4.15 ± 0.75
	8	140 ± 2	269 ± 6	4.11 ± 0.37
	12	159 ± 04	276 ± 4	3.26 ± 0.9
	16	164 ± 09	272 ± 7	3.13 ± 0.11
	24	177 ± 1	298 ± 33	4.16 ± 0.32
505	2	194 ± 1	284 ± 8	2.04 ± 0.4
	4	171 ± 2	280 ± 10	2.91 ± 0.6
	8	152 ± 2	290 ± 2	4.52 ± 0.2
	12	197 ± 6	312 ± 8	3.68 ± 0.5
	16	215 ± 4	316 ± 3	2.89 ± 0.45
	24	216 ± 1	335 ± 5	4.1 ± 0.45
515	2	205 ± 2	320 ± 9	3.21 ± 0.5
	4	179 ± 9	317 ± 2	4.11 ± 0.53
	8	199 ± 2	320 ± 11	3.03 ± 0.65
	12	193 ± 12	318 ± 13	4.31 ± 0.45
	16	206 ± 12	341 ± 10	5.1 ± 0.9
	24	178 ± 5	315 ± 3	5.0 ± 0.36
540	2	147 ± 8	179 ± 11	0.78 ± 0.17
	4	157 ± 2	201 ± 11	1.03 ± 0.29
	8	192 ± 1	220 ± 6	0.66 ± 0.07
	12	128 ± 7	160 ± 8	0.92 ± 0.07
	16	143 ± 4	180 ± 5	1.11 ± 0.24
	24	138 ± 6	188 ± 12	0.86 ± 0.31

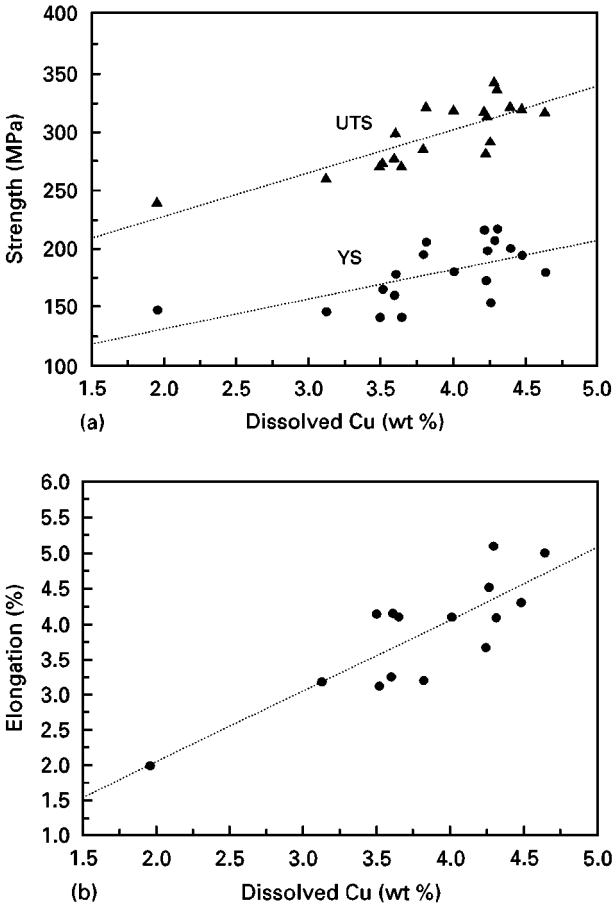

Figure 4 (a) Variation in YS and UTS, (b) variation in El%, as a function of copper concentration in the aluminium matrix.

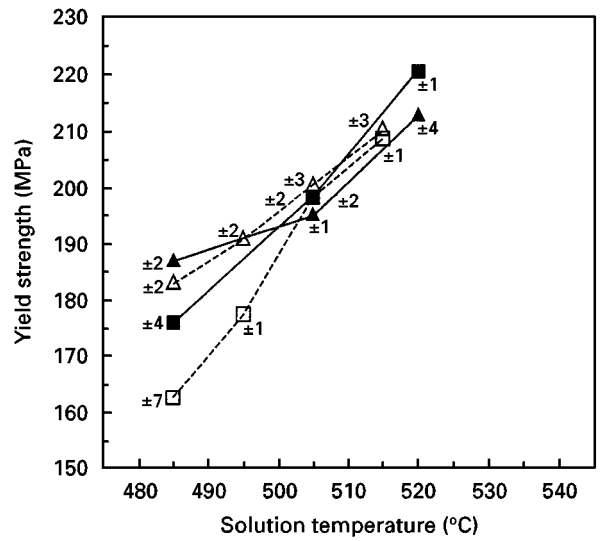

Figure 5 Effect of non-equilibrium solution heat treatment on YS of 0.3 wt % Mg-containing 319 alloy with various amounts of iron and manganese. (△) 1.0% Fe + 0.5% Mn (15 °C s^{-1}), (▲) 1.0% Fe + 0.5% Mn (10 °C s^{-1}), (□) 1.0% Fe (15 °C s^{-1}), (■) 1.0% Fe (10 °C s^{-1}).

3.3.2. Al–Si–Cu–Mg alloys

Tensile test results of test bars prepared from A alloy (containing 0.3 wt %, Mg, with different levels of iron and manganese) that were solution treated at different temperatures are shown in Figs 5–7. The tensile

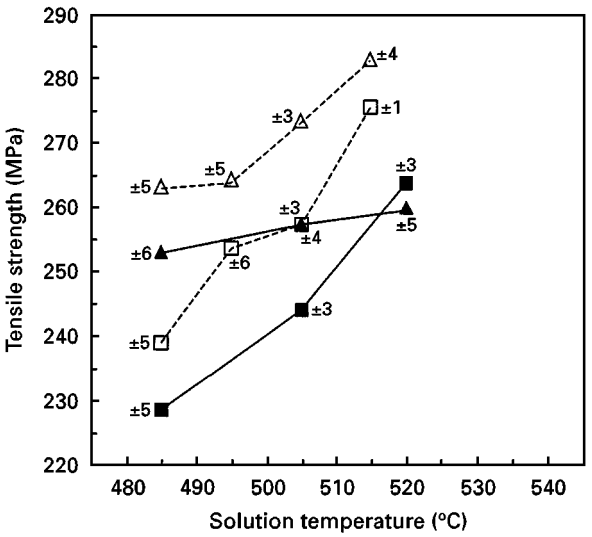

Figure 6 Effect of non-equilibrium solution heat treatment on UTS of 0.3 wt % Mg-containing 319 alloy with various amounts of iron and manganese. (△) 1.0% Fe + 0.5% Mn (15 °C s^{-1}), (▲) 1.0% Fe + 0.5% Mn (10 °C s^{-1}), (□) 1.0% Fe (15 °C s^{-1}), (■) 1.0% Fe (10 °C s^{-1}).

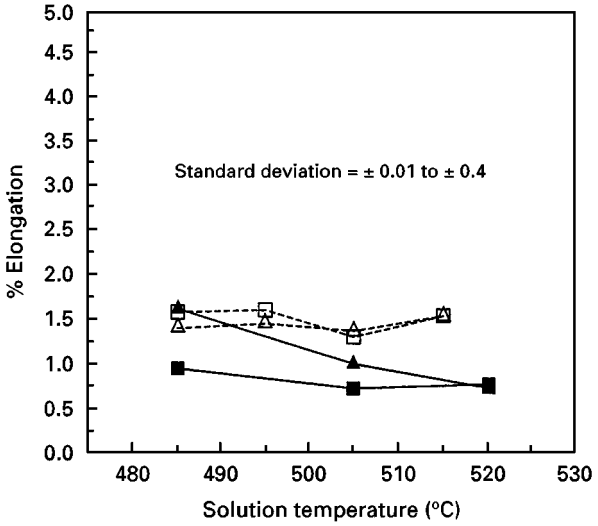

Figure 7 Effect of non-equilibrium solution heat treatment on El % of 0.3 wt % Mg-containing 319 alloy with various amounts of iron and manganese. Note in Figs 5–7, test bars were aged for 5 h at 150 °C after quenching. (△) 1.0% Fe + 0.5% Mn (15 °C s^{-1}), (▲) 1.0% Fe + 0.5% Mn (10 °C s^{-1}), (□) 1.0% Fe (15 °C s^{-1}), (■) 1.0% Fe (10 °C s^{-1}).

strength of all the alloys increases with solution temperature and reaches a maximum value in the optimum solution temperature range of 515–520 °C. At a solution temperature of 535 °C, just 15 °C above the optimum range, the test bars are observed to fail at very low stresses, typically 60–130 MPa. This behaviour is attributed to the generation of a high volume of liquid phases at grain boundaries and in the interdendritic regions.

Fig. 8 summarizes the effect of solution temperature on the average values of YS, UTS and E1% of WM alloy (containing ~0.5 wt % Mg, see Table VI for details of heat treatments). As expected, solution treatment at 510 °C is more appropriate than that at 520 °C. It is also noted that lowering the quenching

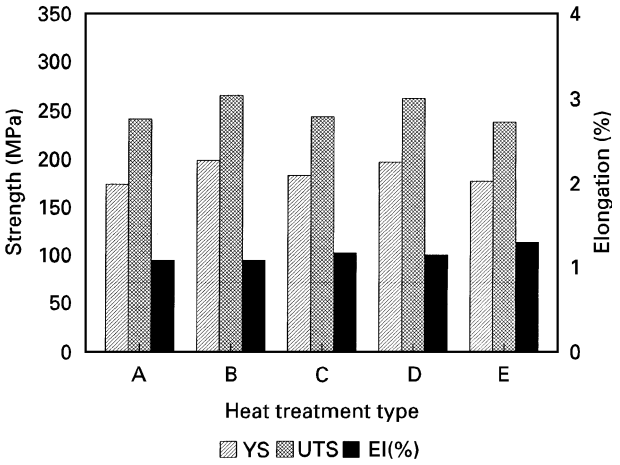

Figure 8 Tensile properties of WM alloy following different solution treatments.

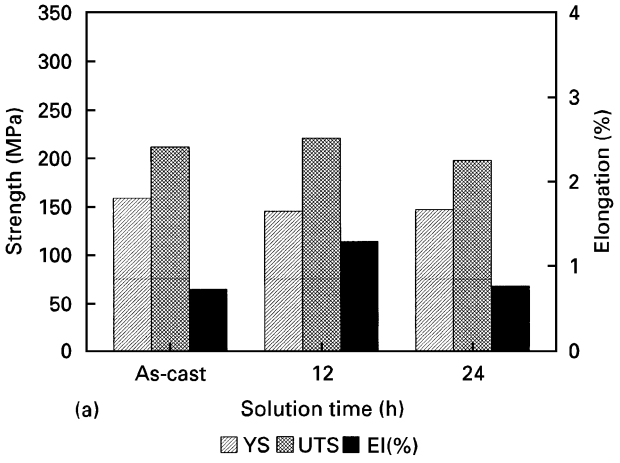

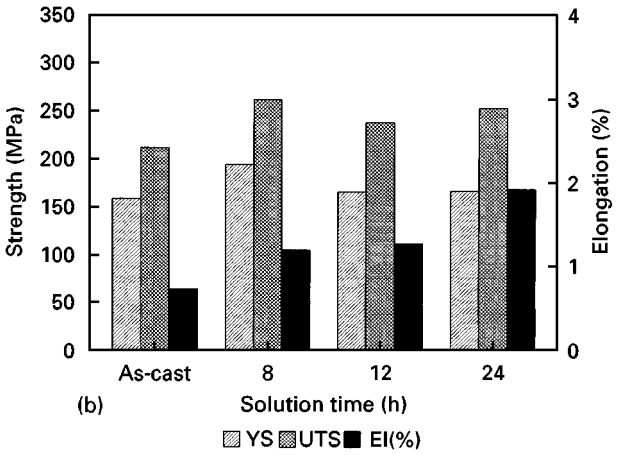

Figure 9 Effect of solution time on the tensile properties of WM alloy solution treated at (a) 480 °C, (b) 510 °C.

TABLE VI Single-stage solution heat treatments followed for G and WM alloys

Code	Details
A	12 h at 480 °C, quenching in hot water.
B	12 h at 510 °C, quenching in hot water.
C	12 h at 510 °C, lowering the temperature to 480 °C, quenching in hot water.
D	12 h at 520 °C, quenching in hot water.
E	12 h at 520 °C, lowering the temperature to 480 °C, quenching in hot water.

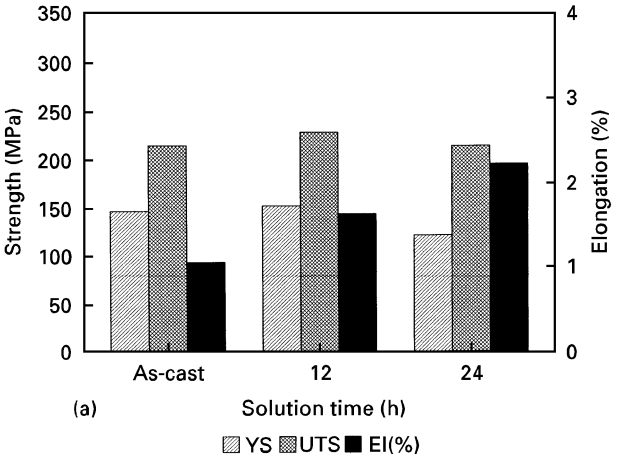

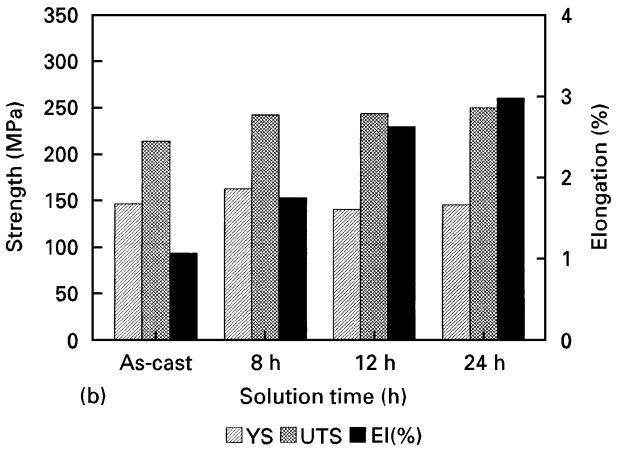

Figure 10 Effect of solution time on the tensile properties of G alloy solution treated at (a) 480 °C, (b) 510 °C. Note in Figs 8–10, test bars were not aged after quenching.

temperature to 480 °C prior to quenching slightly improves the alloy ductility at the cost of alloy strength. To investigate the effect of prolonged solution treatment at 480 °C and 510 °C, several batches (15 test bars per batch) of the high-magnesium version of W alloy, i.e. containing ~0.5 wt % Mg, were heated for times ranging between 8 and 24 h. Fig. 9a reveals that heating at 480 is not very effective in changing the tensile properties of the cast alloy. On the contrary, the alloy exhibits a better response at 510 °C, particularly in terms of ductility, as can be seen from Fig. 9b.

In order to determine more precisely the effectiveness of solution time in improving the tensile properties of the as-cast G alloy (low magnesium content, low volume fraction of intermetallics) test bars of the alloy were treated similarly. At 480 °C, the main role of solution time appeared to be in increasing the alloy ductility without noticeable changes in YS and UTS values (Fig. 10a). Prolonged solution treatment at 510 °C brought about significant changes in UTS and elongation levels (Fig. 10b). The results of tensile testing performed on test bars of alloys with two levels of magnesium content, i.e. 0.05% and 0.5% (i.e. G and WM alloys) are displayed in Fig. 11. The test bars were solution treated for 8 h either at 480 or 500 °C, followed by quenching into hot water (60 °C) and artificial ageing for 5 h at 180 °C thereafter. At low solution-treatment temperature, i.e. 480 °C,

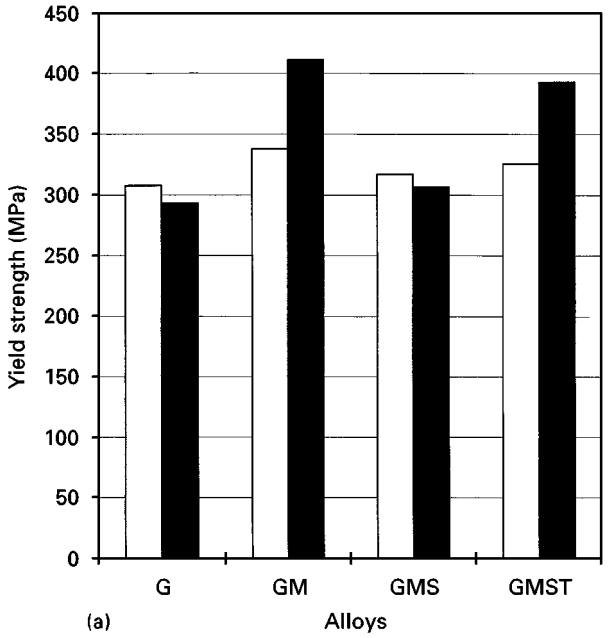

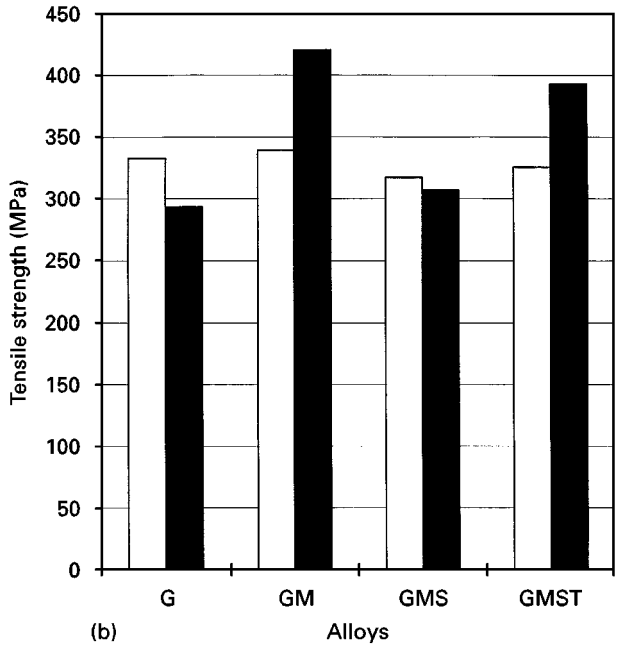

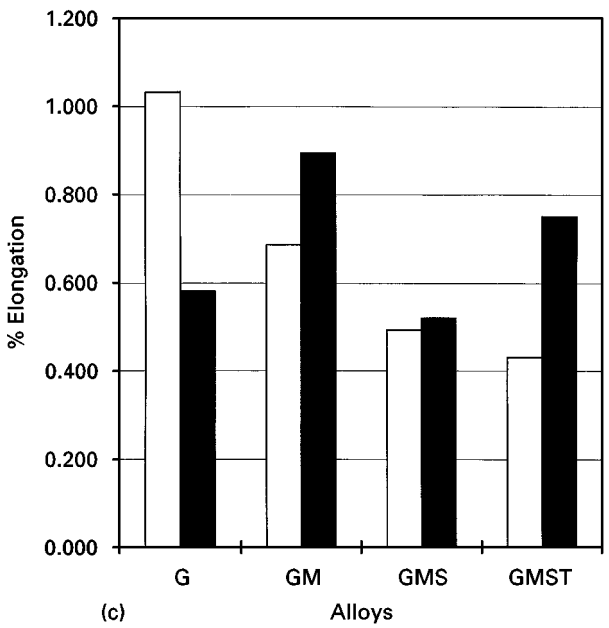

Figure 11 Comparison of tensile properties of G, GM, GMS, GMST alloys solution treated at (□) 480 and (■) 500 °C: (a) YS, (b) UTS, (c) El %. Test bars were aged for 5 h at 180 °C after quenching.

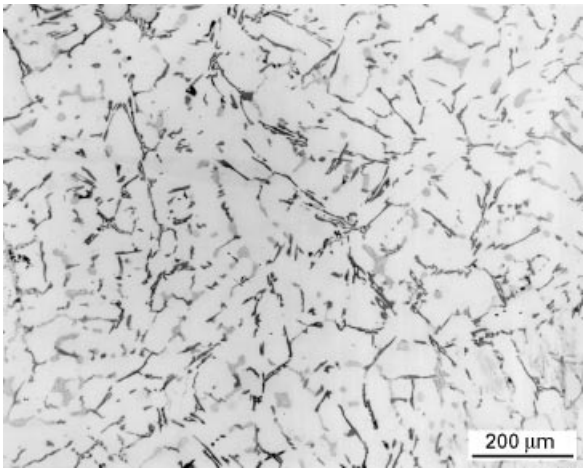

Figure 12 Microstructure of G alloy in the as-cast condition.

magnesium does not seem to provide any significant improvement in the alloy properties. These results may indicate that 480 °C is a fairly low solution-temperature to cause an appreciable solid solution of magnesium and copper in the aluminium matrix. Thus, the ageing response of the alloys is more or less negligible.

When the solution-treatment temperature is raised to 500 °C, a remarkable ageing response is exhibited by the high magnesium-containing alloys, as shown in Fig. 11. The yield and tensile strengths of the GM alloy increase, respectively, from 330 and 340 MPa to 410 and 420 MPa. Also, although the GMST alloy apparently displays slightly lower strength parameters compared to those obtained from the GM alloy, consistency in the data is markedly better. Due to improvement in the silicon particle spheroidization process, coupled with a greater dissolution of the Al_2Cu phase in the aluminium matrix, the ductility of the GM alloy has also increased.

3.4. Microstructure

3.4.1. Al–Si–Cu alloys

During solution heat treatment, incipient melting of a binary alloy can occur when the alloy composition exceeds the critical composition and the alloy is annealed at a temperature higher than the eutectic temperature. In alloys with segregation of the alloying elements, the composition may locally exceed the critical composition, even though the mean composition is lower, and incipient melting again occurs in this case [5].

Fig. 12 shows the as-cast microstructure of G alloy (Mg ~ 0.06 wt %) comprising an α-aluminium dendrite network with eutectic silicon and Al_2Cu particles segregated into the interdendritic regions. The high-magnification micrograph of Fig. 13a reveals

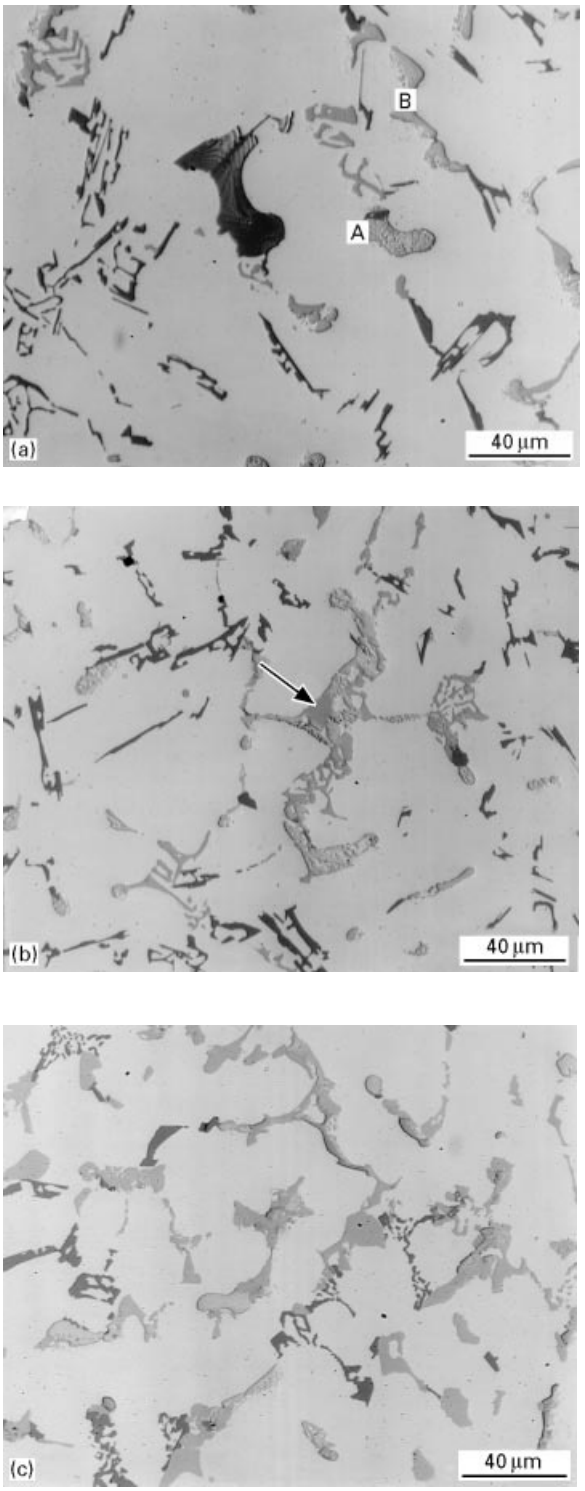

Figure 13 High-magnification micrographs of (a) G, (b) GM, (c) GMS alloys in the as-cast condition.

that the silicon particles (or flakes) are unmodified. However, the relatively higher cooling rate associated with permanent mould casting ($\sim 8\,^{\circ}C\,s^{-1}$, corresponding to a dendrite arm spacing ~ 20–$25\,\mu m$) leads to smaller silicon particles. The Al_2Cu phase precipitates in two distinct morphologies, i.e. ($Al + Al_2Cu$) eutectic and blocky type. The copper concentrations in these two types are, respectively, 28 and 40 wt % [18].

Increasing the magnesium content to ~ 0.45 wt % (GM alloy) results in the formation of thick plates of $Al_5Mg_8Si_6Cu_2$ (dark grey, arrowed) growing out of the Al_2Cu phase particles, Fig. 13b. Modification of the high-magnesium alloys with 300 p.p.m. Sr, i.e. GMS and GMST alloys, leads to two main observations: (a) modification of the eutectic silicon particles and their segregation in the form of isolated colonies, (b) severe segregation of both $Al_5Mg_8Si_6Cu_2$ and Al_2Cu phase particles in areas away from the advancing interfaces of the eutectic silicon colonies, Fig. 13c. As a result of such a segregation, Al_2Cu is mostly in the form of blocky phase with high copper concentrations (~ 38–40 wt %), which makes their dissolution in the aluminium matrix, during solution treatment, very slow. When the G alloy is solution heat treated at temperatures above the melting point of the eutectic ($Al + Al_2Cu$) phase, e.g. $540\,^{\circ}C$, the Al_2Cu particles may undergo incipient melting even after periods as short as 2 min as evidenced by the black spots (arrowed) observed within the Al_2Cu particles shown in Fig. 14a. Fig. 14b displays an example of how rapid coarsening of the ($Al + Al_2Cu$) eutectic takes place after a 2 h solution treatment. Also observed within the eutectic are silicon particles (arrowed). Chinese script α-Fe phase particles are found present in the conglomeration. Fig. 14c shows the micrograph obtained from a sample solution heat treated at $540\,^{\circ}C$ for 8 h, showing how the melting of the Al_2Cu eutectic particles has progressed (outward from the central region of the particle as shown in Fig. 14a), resulting in a liquid drop-like structure form of the phase upon quenching. Traces of the previously existing Al_2Cu eutectic can be observed at the outer edges of the molten phase. Fig. 14d shows the microstructure obtained after solution treatment at $540\,^{\circ}C$ for 24 h, where pieces of the blocky copper phase are still found remaining (arrowed).

3.4.2. Al–Si–Cu–Mg alloys

The microstructure of test bars (GM alloy) solution treated at $480\,^{\circ}C$ (sections were taken from the gauge length away from the rupture surface) reveal: (a) the persistence of the α-aluminium dendritic structure (Fig. 15a), (b) a slight tendency for silicon-particle fragmentation, and (c) the absence of any sign of incipient melting of the copper-base intermetallics, Fig. 15b. Dissolution of Al_2Cu phase is evident when the high magnesium-containing alloys are solution treated at $500\,^{\circ}C$ ($5\,^{\circ}C$ below the first melting point in GM alloy, Fig. 2), leaving behind tiny particles, circled in Fig. 16a. Thick plates of $Al_5Mg_8Si_6Cu_2$ are still seen, Fig. 16b, whereas blocky particles of Al_2Cu phase in GMS alloy are yet undissolved, Fig. 16c. A dramatic change in the microstructure of GM alloy is seen when the test bars are solution heat-treated at $505\,^{\circ}C$: (a) replacement of the α-aluminium dendritic network by an equiaxed grain structure, (b) segregation of silicon and copper intermetallic particles to the grain boundaries, and (c) localized grain-boundary melting, Fig. 17a. The arrow in Fig. 17a indicates the presence of the unmelted fragments of copper-phases attached to the liquid phase. Modification with strontium did not bring about any particular changes, as shown in Fig. 17b.

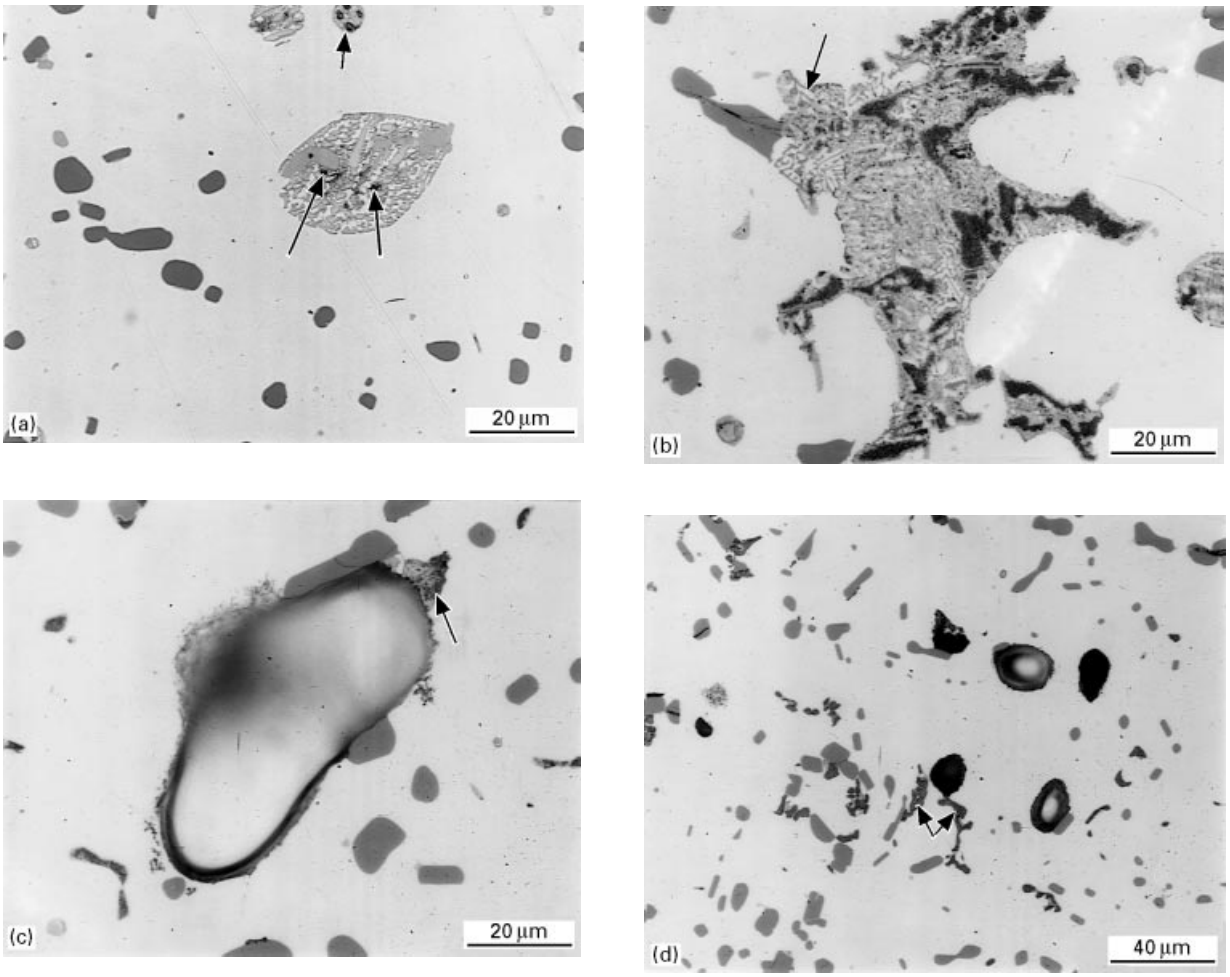

Figure 14 Melting process of Al_2Cu phase in samples solution heat-treated at 540 °C: (a) initiation of melting (arrowed) in a sample heated up to 540 °C and quenched immediately; (b) after 2 h, showing massive Al_2Cu coexisting with silicon and α-iron phases; (c) after 8 h, showing the structureless phase – note the presence of the previously existing Al_2Cu eutectic at the outer fringes (arrowed); and (d) after 24 h, showing the presence of cavities and structureless phase particles – note the presence of the undissolved blocky Al_2Cu phase (arrowed).

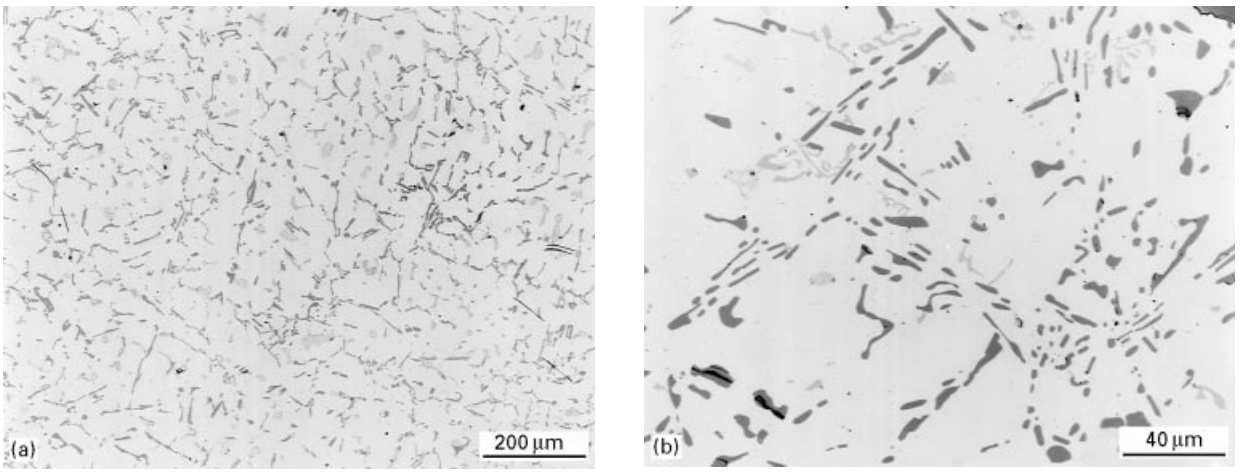

Figure 15 Microstructure of GM alloy solution treated at 480 °C: (a) low magnification, (b) high magnification.

In A alloy (containing ~0.3 wt % Mg), melting starts at grain boundaries and in the interdendritic regions at temperatures below 520 °C, as shown in Fig. 18a. The copper intermetallics, present in bulk form, melt at solution temperatures above 500 °C, leading to the formation of spherical liquid droplets within the dendrites/grains as shown in Fig. 18b. At high solution temperature (535 °C), the width of the grain-boundary melted zone increases, and the spherical interdendritic liquid droplets enlarge and coalesce to form a large network of interdendritic liquid, Fig. 18c.

Another series of test bars were solution treated in two-stages, i.e. 12 h at 510 °C followed by another 12 h at T °C, prior to quenching in hot water (60 °C). Fig. 19 compares the colour of the outer surfaces of test bars solution heat treated following the two-stage process, with the temperature of the second stage,

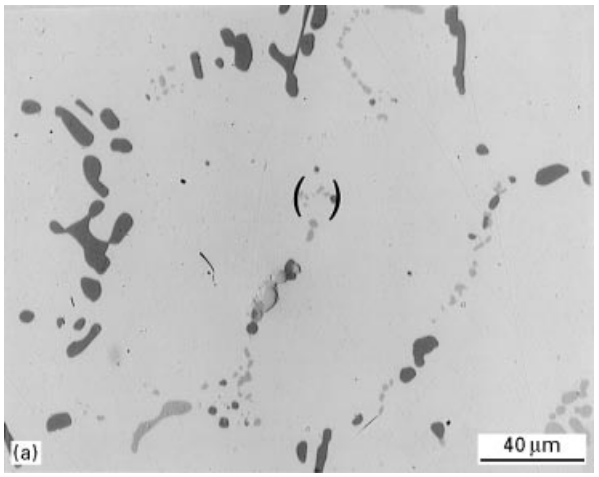

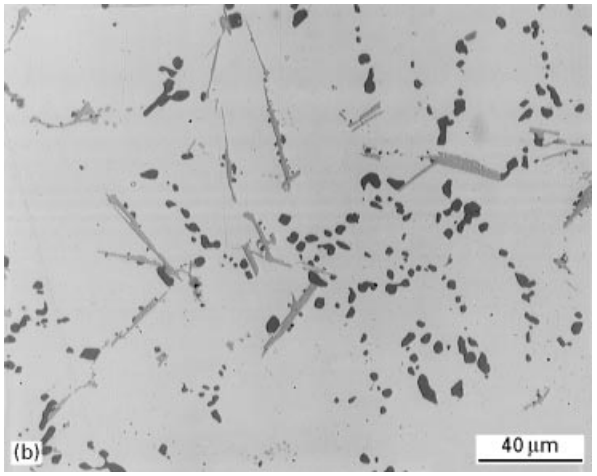

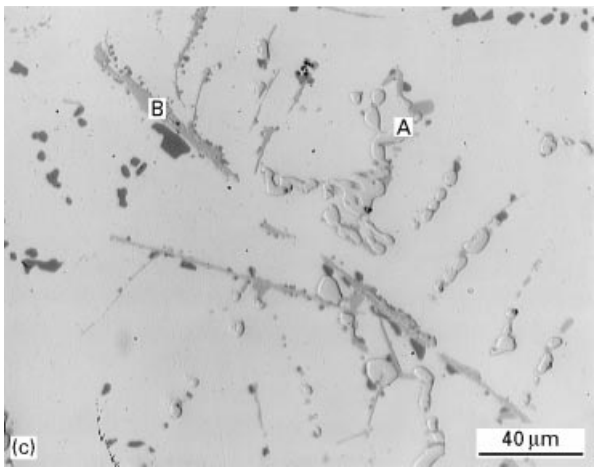

Figure 16 Microstructure of test bars solution treated at 500 °C: (a) G, (b) GM, (c) WMS alloys. Note the presence of Al_2Cu in blocky form (marked A) and $Al_5Mg_8Si_6Cu_2$ (marked B) phase particles.

T °C, varied between 510 and 540 °C (10 °C interval), and for two different levels of magnesium, i.e. 0.06 and 0.5 wt %. Low magnesium-containing test bars, Fig. 19a, exhibit more or less shiny skins. The degree of brightness, however, is much lower (see sample labelled F) compared to that of as-cast test bars (see sample labelled A). In contrast, test bars containing 0.5 wt % Mg reveal a clear tendency for "burning" once the solution temperature has exceeded 520 °C,

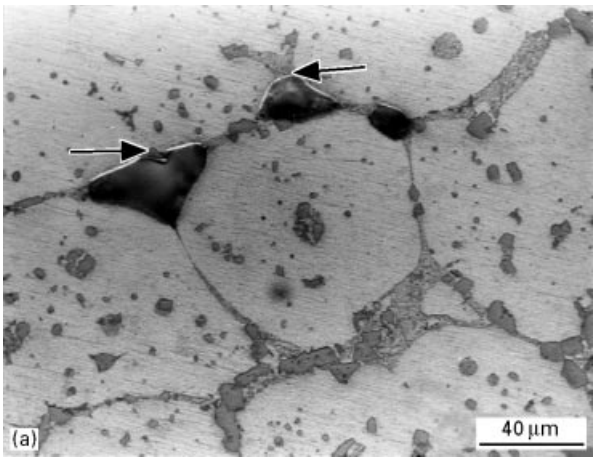

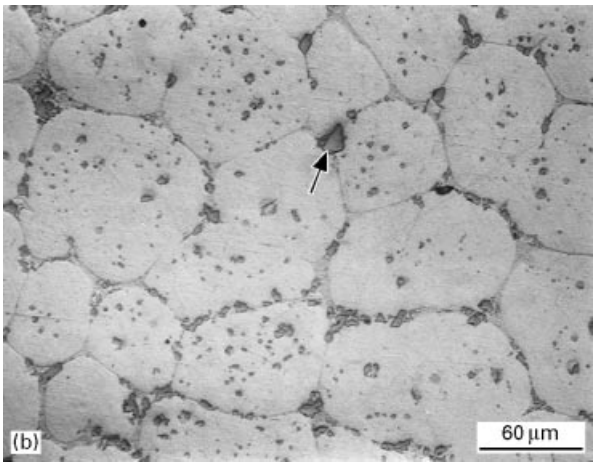

Figure 17 Incipient melting of copper-base intermetallics at the grain boundaries for samples solution treated at 505 °C: (a) GM, (b) GMS alloys.

with a marked distortion when the temperature is raised to 540 °C (see sample labelled F, Fig. 19b). The essential rupture features inferred from the broken test bars (G alloy, 0.06 wt % Mg) in the as-cast as well as solution heat-treated (two-stage treatment, 12 h/150 °C + 12 h/540 °C) conditions, are shown in Fig. 20a and b. In both cases, ductile rupture is the main fracture mechanism. Cracks were initiated at the centres of the test bars, followed by their propagation towards the outer surface.

The fracture details of high magnesium-containing test bars (WM alloy) depend chiefly on the type of heat treatment and, in particular, the temperature of the second stage. Up to 520 °C, broken test bars reveal a similar surface quality (bright, defect free, Fig. 21b) compared with that obtained from as-cast test bars pulled to rupture (Fig. 21a). At a higher solution treatment temperature, i.e. 530 °C, a ring of black spots caused by "burning" or "fusion" of the copper intermetallics was observed close to the outer surfaces, for all test bars (Fig. 21c), that expanded into the centres of the broken test bars when the temperature was further raised to 540 °C (Fig. 21d). This observation was strongly related to the magnesium concentration, regardless of the type of base alloy (i.e G or W), and caused complete distortion of all the test bars.

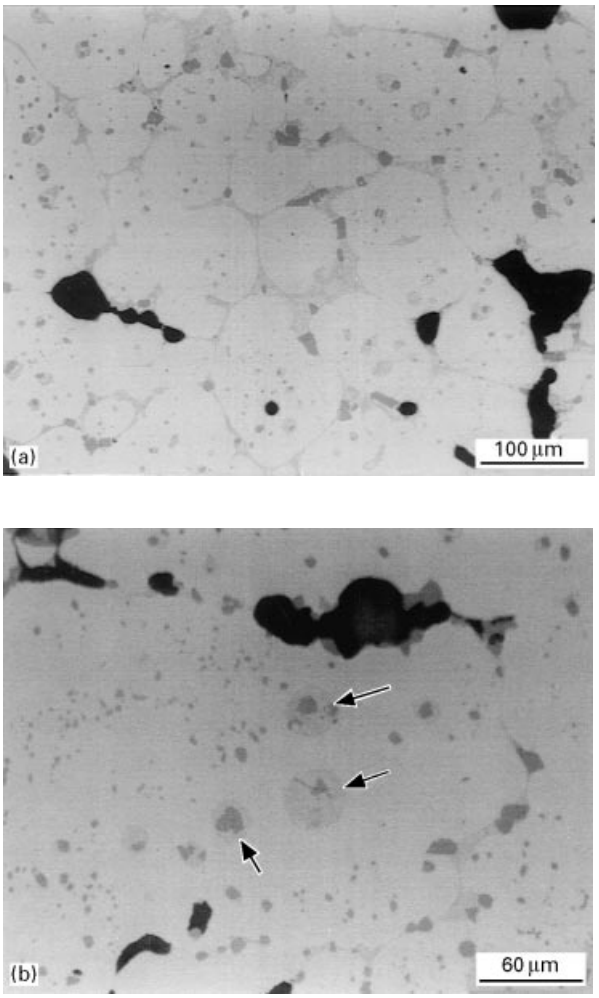

Figure 18 Incipient melting of copper-base intermetallics in A alloy for samples solution treated at (a) 520 °C (interdendritic and grain-boundary melting), (b) 520 °C (melted droplets); (c) 535 °C (shrinkage porosity developed due to sudden quenching of the liquid copper-phases).

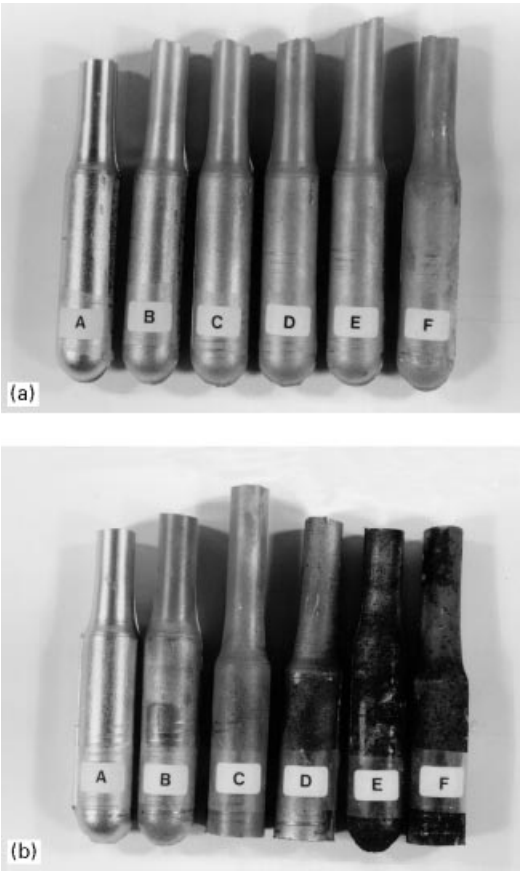

Figure 19 Changes in the degree of brightness of test bars solution heat-treated for 12 h at 510 °C followed by another 12 h at different temperatures (labelled A–F) : (a) 0.06 wt % Mg, (b) ~0.5 wt % Mg. A, as-cast; B, 510 °C; C, 520 °C; D, 525 °C; E, 530 °C; F, 540 °C.

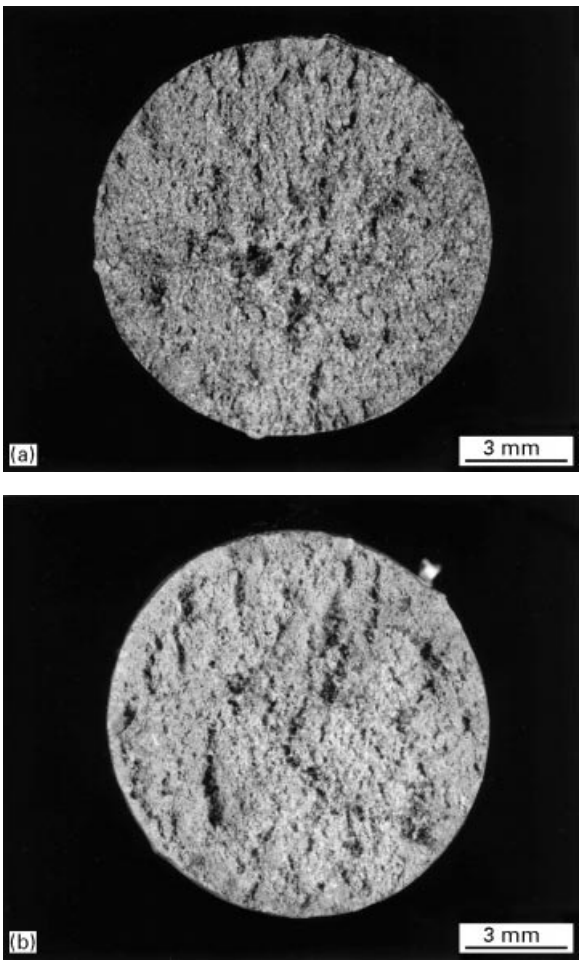

Figure 20 Fracture surfaces of broken test bars of G alloy (a) in the as-cast condition, (b) solution treated for 12 h/510 °C + 12 h/540 °C. Note the absence of molten phases in (b).

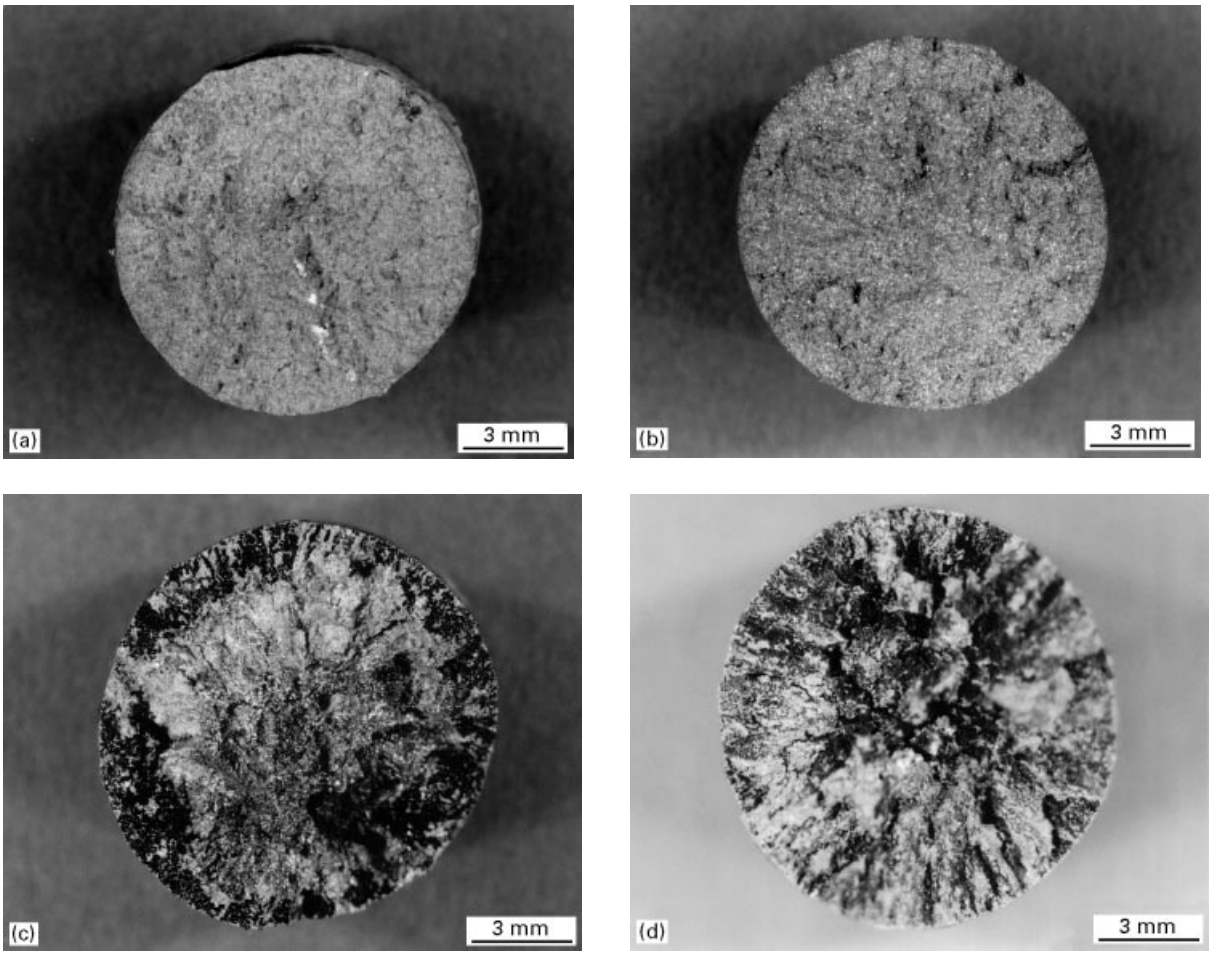

Figure 21 Fracture surfaces of broken test bars of WM alloy (a) in the as-cast condition, (b) solution treated for (12 h/510 °C + 12 h/510 °C), (c) solution treated for (12 h/510 °C + 12 h/530 °C), (d) solution treated for (12 h/510 °C + 12 h/540 °C).

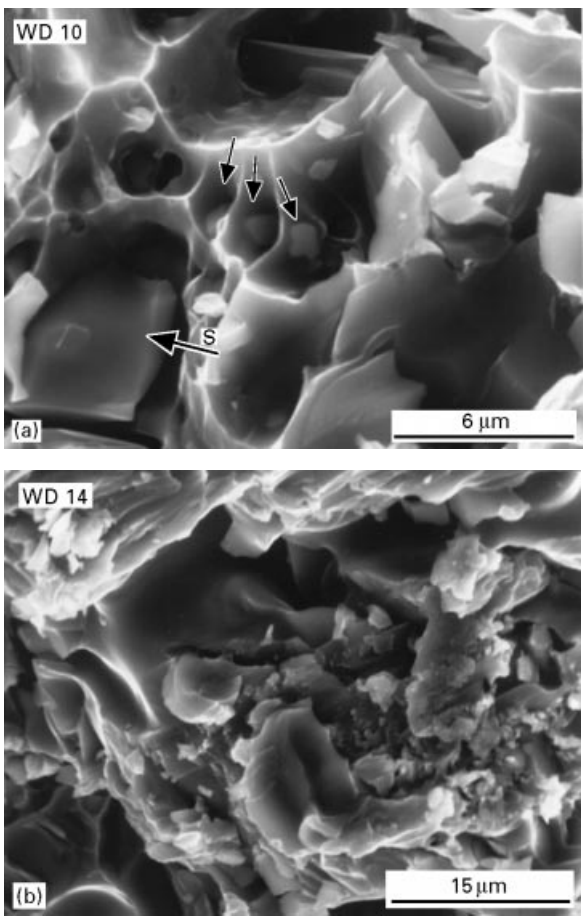

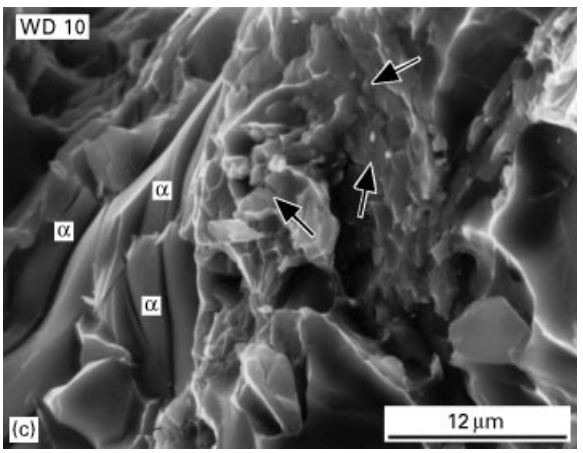

Figure 22 Fracture of (a) Al_2Cu undissolved particles, (b) a mixture of Al_5Mg_8 Si_6Cu_2 and Al_2Cu fragments, (c) fine $Al_5Mg_8Si_6Cu_2$ particles adjacent to α-$Al_{15}(Fe,Mn)_3$ Si_2 Chinese script (marked α).

3.5. Fractography

The effect of the addition of magnesium or (Mg + Sr) on the fracture behaviour of $Al_5Mg_8Si_6Cu_2$ and Al_2Cu intermetallics, when the test bars were solution heat treated for 8 h at 500 °C, is illustrated in Figs 22–26.

Traces of undissolved Al_2Cu particles in W alloy are seen at the bottom of the dimpled structure in Fig. 22a. Their approximate chemical composition

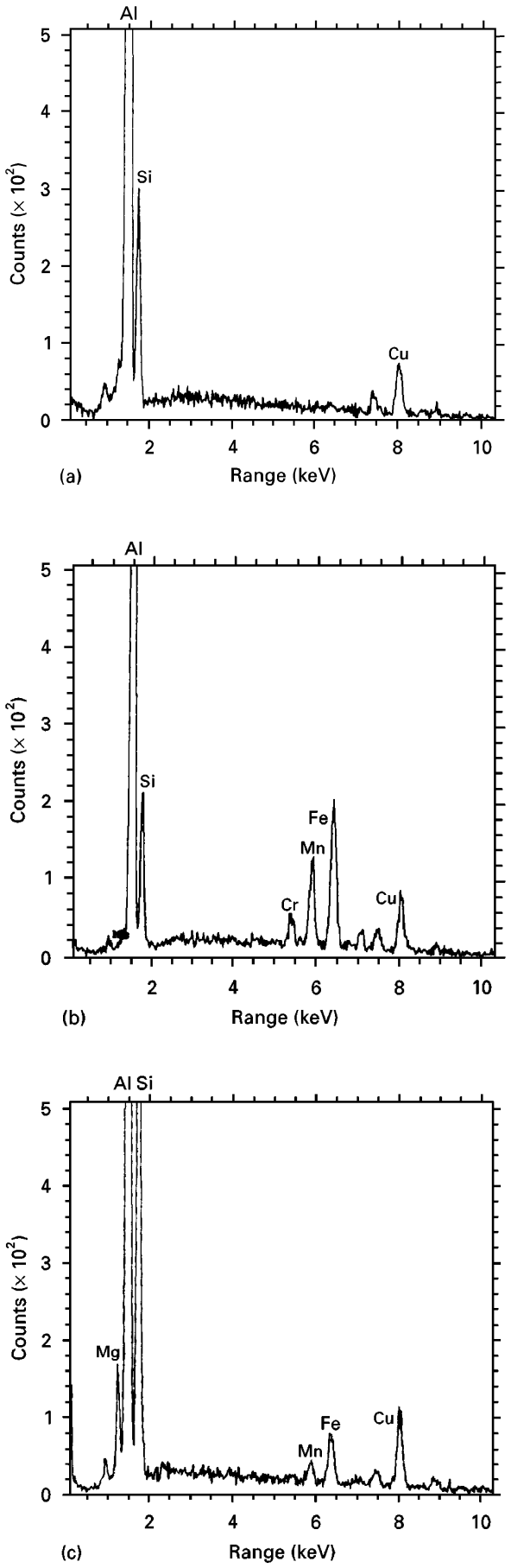

Figure 23 EDX spectra showing (a) Al_2Cu phase, (b) a mixture of Al_2Cu and $Al_{15}(Fe, Mn, Cr)_3 Si_2$ phases, (c) a mixture of $Al_5Mg_8Si_6Cu_2$ and $Al_{15}(Fe, Mn)_3 Si_2$ phases.

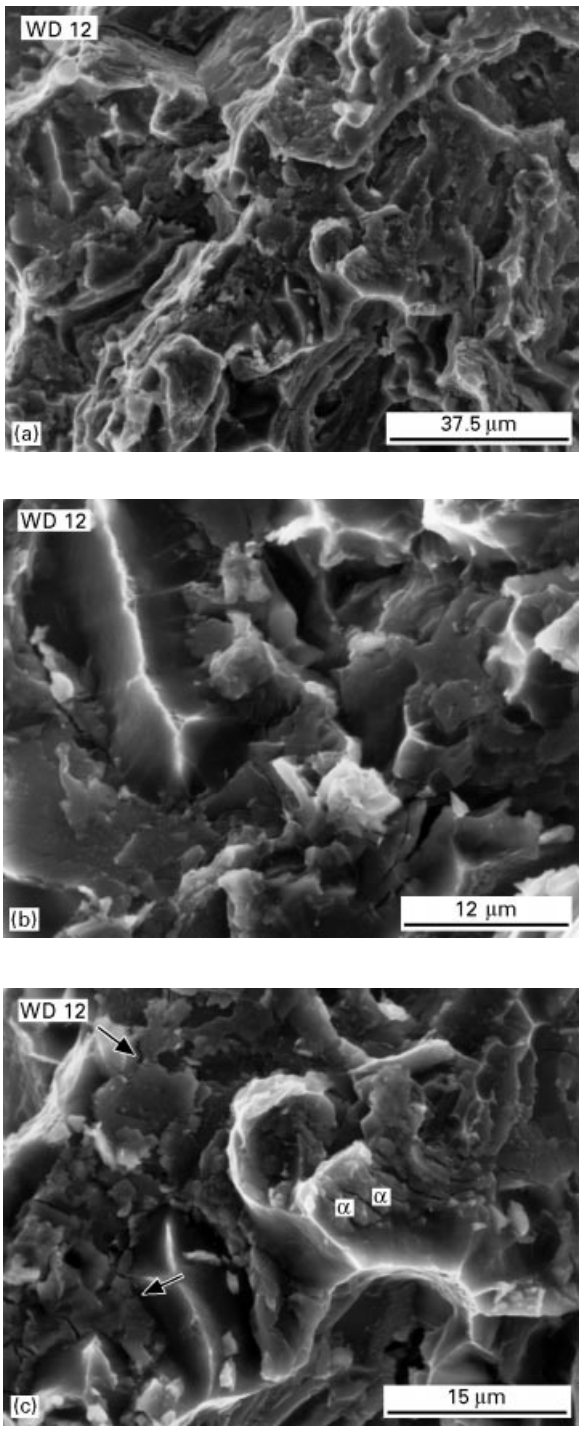

Figure 24 Fracture of (a) a massive area of Al_2Cu and $Al_5Mg_8Si_6Cu_2$ phases, (b) fragmentation of Al_2Cu, (c) fragmentation of $Al_5Mg_8Si_6Cu_2$. Note the irregular shape of the broken pieces.

was confirmed using energy dispersive X-ray (EDX) analysis, as shown in Fig. 23a. In conjunction with these particles, fragments of α-Fe (sludge marked S) are observed. The corresponding EDX spectrum, Fig. 23b, exhibits reflections due to iron, manganese, and chromium elements, indicating that this phase is close to $Al_{12}(Fe, Mn, Cr)_3Si_2$ [2]. Fig. 22b displays the fracture of $Al_5Mg_8Si_6Cu_2$-phase platelets into a large number of small pieces in WM alloy. The associated spectrum, Fig. 23c, exhibits a strong reflection of magnesium. This observation may indicate the progress of dissolution of the $Al_5Mg_8Si_6Cu_2$ phase at 500 °C.

As the solution temperature is relatively low to avoid incipient melting of this intermetallic, prolonged solution times may be required to ensure complete dissolution of this phase in the aluminium matrix which would then render the alloy its maximum strength during artificial ageing thereafter. Of particular interest is the presence of $Al_5Mg_8Si_6Cu_2$ fragments (arrowed), observed at the interfaces of the iron-intermetallic phase (marked α in Fig. 22c). As mentioned earlier, magnesium has a tendency to segregate both copper and iron intermetallics in areas away from the eutectic silicon. The absence of a chromium reflection in Fig. 23c may suggest that the intermetallic phase is α-$Al_{15}(Fe, Mn)_3Si_2$ Chinese script.

Segregation of intermetallics was more pronounced when the high magnesium-containing alloys were modified with $\sim$300 p.p.m. Sr, as evinced in Fig. 24a, which shows a massive area of fractured copper intermetallics. The high-magnification micrograph of Fig. 24b reveals the breakdown of the blocky Al_2Cu phase into several segments. The corresponding EDX spectrum, Fig. 25a, however, displays a weak magnesium reflection caused by the growth of the $Al_5Mg_8Si_6Cu_2$ phase from the Al_2Cu phase during the last stages of solidification. Fracture of a platelet of $Al_5Mg_8Si_6Cu_2$ phase into smaller pieces is shown in Fig. 24c. Note the irregular shape of the edges caused by the progress of dissolution. In this case, a notably strong reflection due to magnesium is seen in Fig. 25b. It is interesting to note that its intensity is higher than that of the copper reflection. This observation may suggest the presence of undissolved Mg_2Si.

For a clear understanding of the effect of solution heat treatment on the fragmentation of copper-base

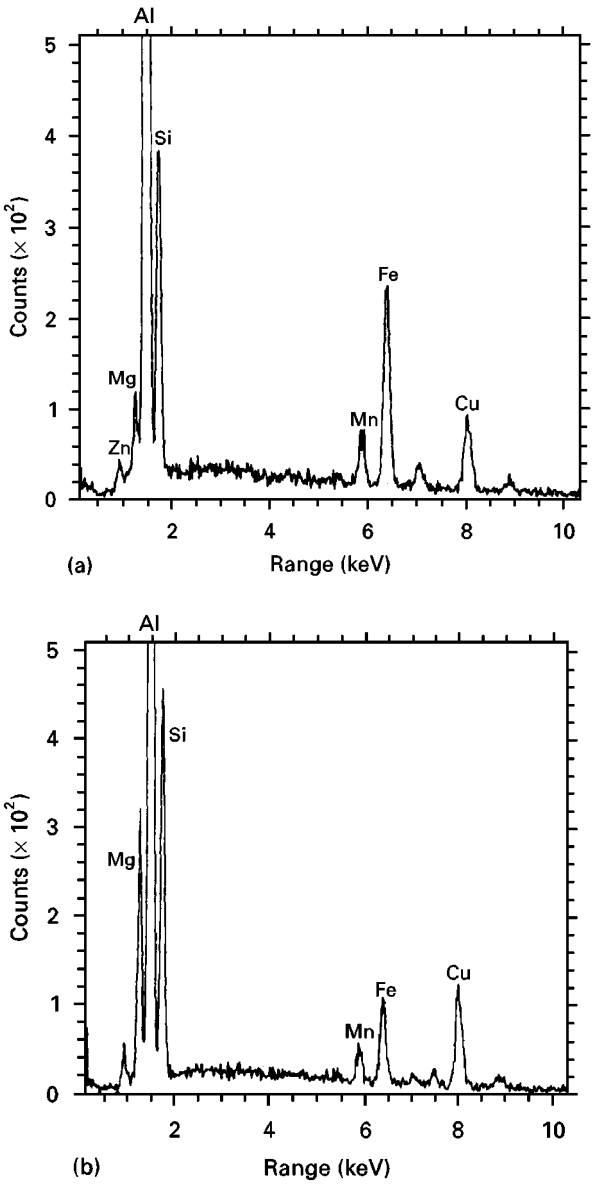

Figure 25 EDX spectra showing a mixture of Al_2Cu, $Al_5Mg_8Si_6Cu_2$, and $Al_{15}(Fe,Mn)_3Si_2$: (a) weak magnesium reflection, (b) strong magnesium reflection.

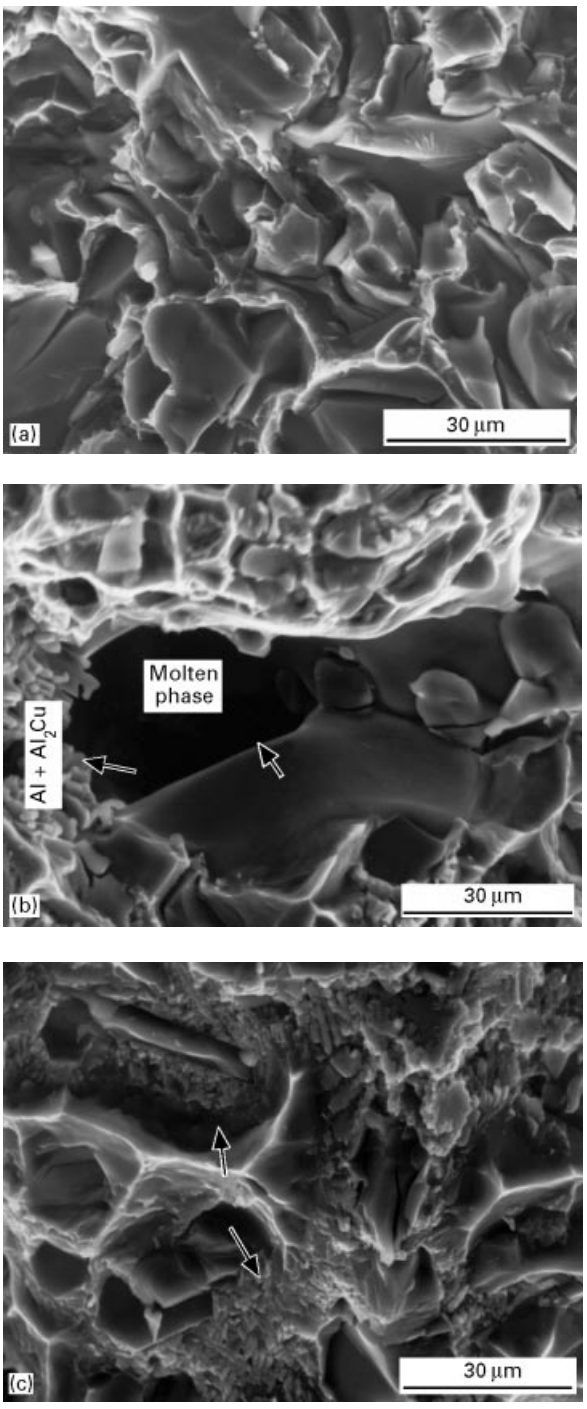

Figure 26 Fractographs of (a) blocky Al_2Cu phase in the as-cast condition, (b) incipient melting of copper intermetallics, (c) massive conglomerated areas of (Al + Al_2Cu) eutectic.

intermetallics, Fig. 26a exhibits the fracture of blocky Al_2Cu in GMS alloy in the as-cast condition. Two main observations can be made: (i) the number of fragments is lower than that seen in Fig. 24a and the fragments have much larger sizes, (ii) the edges of these fragmented particles are much smoother than those shown in Fig. 24. In contrast, when the alloys (e.g. G alloy) are solution heat treated at temperatures above the incipient melting temperature of the Al_2Cu phase, large voids (Fig. 26b) or massive conglomerated areas of ($Al + Al_2Cu$) eutectic (Fig. 26c) are seen on the fractured surface.

4. Conclusions

4.1. Al–Si–Cu alloys (Mg ~0.04 wt %)

1. Dissolution of the eutectic ($Al + Al_2Cu$) takes place at temperatures close to the final solidification temperature of the alloy (i.e. 480 °C), the dissolution accelerating with increasing solution temperature. Melting of the eutectic copper phases is observed at a solution temperature of ~540 °C.

2. The tensile strength and elongation properties (of test bars solution heat treated at 480–515 °C for 2–24 h) show a linear increase when plotted against the amount of dissolved copper in the matrix. The yield strength is not affected by the dissolution of the Al_2Cu phase, indicating that this property is not controlled by copper dissolution.

4.2. Al–Si–Cu–Mg alloys (Mg ~0.3–0.5 wt %)

1. Non-equilibrium heat treatments increase the strength properties. The optimum solution-treatment temperature is found to be 500–520° C.

2. Magnesium up to ~0.5 wt % contributes to both strength parameters, i.e. YS and UTS, by about 75%, and alloy ductility by about 15%. A single-stage treatment consisting of solution treatment at 500–510 °C for 12 h may be recommended. This process should be followed by artificial ageing for 2–5 h at 160–180 °C. Overageing does not bring about much change in the tensile properties.

3. Incipient melting of $Al_5Mg_8Si_6Cu_2$ and Al_2Cu phases takes place when the high-magnesium version of 319 is solution treated at temperatures above 505 °C for sufficiently lengthy periods; this results in distortion of the test bars (i.e. casting) and deterioration of the alloy mechanical properties.

4. Fracture of both $Al_5Mg_8Si_6Cu_2$ and Al_2Cu intermetallics occurs through their fragmentation into small particles. These particles have irregular interfaces caused by their progressive dissolution in the aluminium matrix.

Acknowledgements

Financial support received from the Natural Sciences and Engineering Research Council of Canada (NSERC), the Fondation de l'Université du Québec à Chicoutimi (FUQAC) and the Centre Québécois de recherche et de développement de l'aluminium (CQRDA) is gratefully acknowledged.

References

1. D. APELIAN, S. SHIVKUMAR and G. SIGWORTH, *AFS Trans.* **97** (1989) 727.
2. L. BACKERUD, G. CHAI and J. TAMMINEM, *Solidif. Charact. Alumin. Alloys* **2**, Foundry Alloys, AFS/skan aluminium, Des Plaines, IL, USA (1990) 71.
3. "*Special Report on the Mechanical Properties of Permanent Mold Aluminium Test Casting*", (The Aluminium Association, 1990).
4. O. REISO, N. RYUM and J. STRID, *Metall. Trans.* **24A** (1993) 2629.
5. O. REISO, H. G. VERLIE and N. RYUM, *ibid.* **21A** (1990) 1689.
6. Y. AWANO and Y. SHIMIZU, *AFS Trans.* **98** (1990) 889.
7. J. E. HATCH (ed.), "*Aluminium: Properties and Physical Metallurgy*", (ASM, Oh, 1964).
8. P. ARCHAMBAULT *et al.*, in "*Optimum Quenching Conditions for Aluminium Alloy Castings, Heat Treatment* 1976", Proceedings of the 16th International Heat Treatment Conference, (Metals Society, London, 1976), Book 181, p. 105–109.
9. J. GAUTHIER, P. R. LOUCHEZ and F. H. SAMUEL, *Cast Metals* **8** (1995) 91.
10. J. GAUTHIER, P. R. LOUCHEZ and F. H. SAMUEL, *ibid.* **8** (1995) 114.
11. A. M. SAMUEL, J. GAUTHIER and F. H. SAMUEL, *Metall. Mater. Trans. A* **27A** (1996) 1785.
12. L. ANANTHA NARAYANAN, F. H. SAMUEL and J. E. GRUZLESKI, *ibid.* **26A** (1995) 2161.
13. P. OUELLET, F. H. SAMUEL, D. GLORIA and S. VALTIERRA, *Int. J. Cast Metal. Res.* **10** (1997) pp. 67–78.
14. H. de la SABLONNIÈRE and F. H. SAMUEL, *ibid.* **9** (1996) 195.
15. H. de la SABLONNIÈRE and F. H. SAMUEL, *ibid.* **9** (1996) 213.
16. A. M. SAMUEL, P. OUELLET, F. H. SAMUEL and H. W. DOTY, *AFS Trans.* **105** (1997) 951–962.
17. S. SHIVKUMAR, S. RICCI, JR, B. STEENHOFF and D. APELIAN, *AFS Trans.* **98** (1990) 913.
18. A. M. SAMUEL, H. W. DOTY and F. H. SAMUEL, *J. Mater. Sci.* **31** (1996) 5529.

Received 9 July
and accepted 17 December 1997